DE88015481



# HEAT TRANSFER INVESTIGATIONS IN A SLURRY BUBBLE COULMN: QUARTERLY REPORT OF THE PERIOD JANUARY--MARCH 1988

ILLINOIS UNIV. AT CHICAGO CIRCLE. DEPT.
OF CHEMICAL ENGINEERING

1988

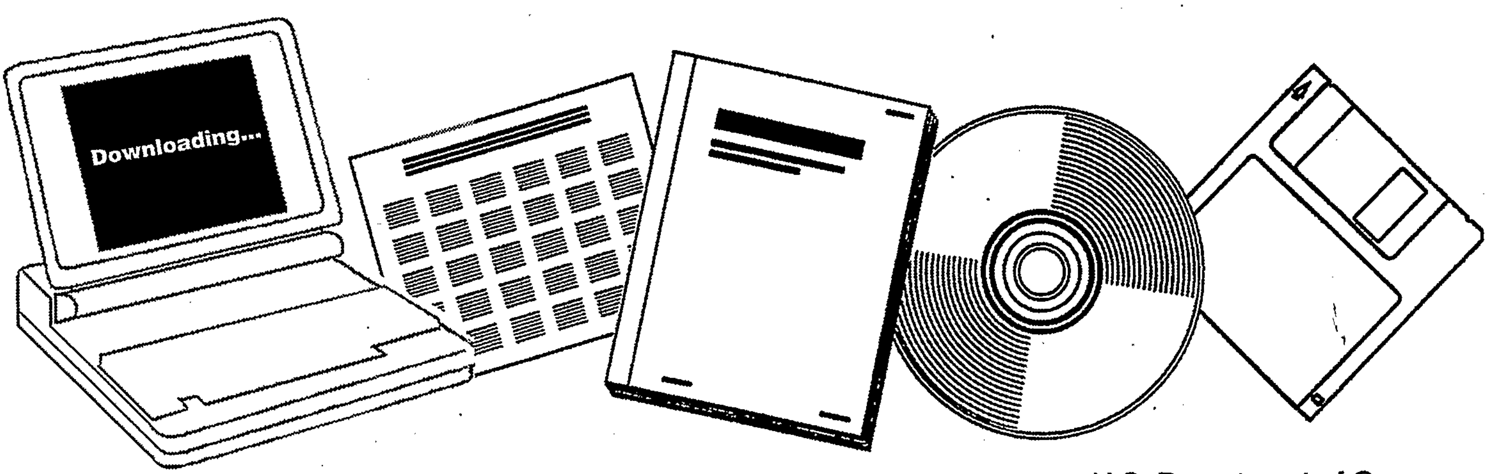


U.S. Department of Commerce
**National Technical Information Service**

DOE/PC/90008--T3

DE88 015481

# HEAT TRANSFER INVESTIGATIONS IN A SLURRY BUBBLE COLUMN

Quarterly Report of the Period January - March 1988

S.C. Saxena, Principal Investigator
R. Vadivel, Research Associate
A.K. Verma, Research Associate

University of Illinois at Chicago
Department of Chemical Engineering
810 South Clinton, Chicago, IL 60607



Prepared for the United States Department of Energy, Pittsburgh Energy Technology Center, Under DOE Contract No. DE -AC22-86 PC 90008
DOE Project Manager: Mr. George Cinquegrane

## OBJECTIVES

To investigate the heat transfer characteristics in two slurry bubble columns (Diameters 10.8 and 30.5 cm) as a function of system and operating parameters.

## SUMMARY

The small 10.8 cm diameter Plexiglas slurry bubble column has been operated in various modes and in different environment. It has been used to measure heat transfer coefficient between a heat transfer probe of 19 mm diameter placed coaxially and air-water dispersion as a function of air velocity. The effect of water flow velocity, position of heat-transfer section and heat flux value on heat-transfer coefficient has been studied and discussed. The uncertainty in the measurements have been determined. To study the heat transfer mechanism experiments were conducted to measure fluctuating heat-transfer coefficient at a sampling rate of 10 readings per minute. The experiments were also conducted to measure the local temperature on heat transfer surface at a high sampling rate of 20 readings per second.

The design, fabrication and installation work on the larger 0.305 m diameter column has progressed and it is expected that various flow loops and measuring circuits will be completed shortly. A heat transfer probe of 19 mm diameter is in the advanced stage of fabrication. A special circuit is assembled to energize the electrical heater.

Interpretation of our experimental air holdup data for different operating conditions in terms of available correlations are presented.

## DESCRIPTION OF TECHNICAL PROGRESS

### TASK 2

On the small 10.8 cm diameter Plexiglas column heat transfer data have been taken with heater location in the lower, middle and upper regions of the column. The measurements have been repeated for the middle region of the column to check the reproducibility of the data and hence the precision of our reported heat transfer coefficient, $h_W$, values. All these data are taken in the batch mode as a function of air velocity. The computed $h_W$ values are plotted and are discussed in the following.

To measure the radial temperature distribution in the air-water dispersion, a thermocouple probe with six thermocouples is used. To scan the complete temperature profile at a particular axial location about 20 seconds are needed. The measured temperature profiles are shown in Figure 1 for four values of the air velocity. It is clear that the temperature distribution is very steep at the probe surface and attains a constant value within a distance of a few mm from the probe surface. We have measured the column temperature at the distances of 20, 25 and 30 mm from the probe surface and its mean value is used in calculating the $h_W$ values. However, the column temperature does exhibit a fluctuation at each radial position and it is dependent on the value of air velocity. Thus, at 3.39 cm/s, the temperature fluctuations are almost always within ± 0.25K, while at higher gas velocities the fluctuations reduce to about half of the value at the lower gas velocity i.e., ± 0.12K. These estimates are essential to determine the accuracy of our measured $h_W$ values.

With heater in the middle region of the column i.e., its middle point is 87.5 cm above the air distributor plate, the measured $h_W$ values as a function of time for different air velocities are shown in Figure 2. A repeat run of these measurements is shown in Figure 3. Measured values of $h_W$ in the lower region when the heat transfer probe is located 57.2 cm above the air distributor plate are plotted in Figure 4. Similar data when the heater is located in the upper region with its middle point 118.1 cm above the distributor plate are graphed in Figure 5.

During the measurement of $h_W$ as a function of time, the column temperature changes. The temperature variation is more if the air velocity is low. The approximate column temperatures at various instants are listed in Figures 2-5 at each air velocity. In these figures, it is noticed that when the column temperature is constant $h_W$ assumes its steady state value within a few minutes, less than four minutes and more like two minutes. The rising $h_W$ values with time, particularly evident at lower air velocities, is attributed to the rising temperature of the air-water suspension in the column.

The steady-state $h_W$ values at about 315K as read from Figures 2-5 are listed in Table 1. Also shown in this table are the average air holdup values determined along with the heat transfer measurements. The same data are displayed in Figure 6. It is seen that the $h_W$ values increase with the increase in the air velocity initially but then attain a constant value for higher air velocities greater than about 25 cm/s. The scatter in the $h_W$ values is generally less than ± 2 percent and therefore it is inferred that the variation of $h_W$ along the axis of the column is negligibly small and can be neglected at least for operating conditions and system parameters corresponding to those of Figure 6.

The average air holdup values of Figure 6 indicate a uniform increase in their values with gas velocity over the entire range. In the higher air velocity range, $h_W$ is constant while $\bar{\epsilon}_g$ increases with U. It will suggest that the heat transfer process for these conditions is not sensitively dependent upon the proportion of air in the air-water suspension. This gives us an important clue in the development of the overall heat transfer mechanism from an immersed surface in a two-phase (gas-liquid) suspension.

A series of experiments has been conducted to establish the influence of water flow velocity on $h_w$. Since $h_w$ does not vary along the height of the column, these measurements were taken with the heater located in the middle region of the column. The measured $h_w$ values as a function of time for the water flow velocity of 6.8 mm/s are shown in Figure 7 for three air velocities in the range of our interest where the air-water suspension is in the churn-turbulent regime. Because not enough heat is removed from the system by the exiting gas, the column temperature exhibits a slow increase with time. The heat removed by circulating water is also small due to its low flow rate. In the figure several values of column temperature are shown in each case. In the light of our earlier discussion the $h_w$ values shown in the figure should be regarded as steady-state values.

Similar results as reported in Figure 7 are presented in Figure 8 for water flow velocity of 11.9 mm/s. These results are quite similar to those given in Figure 7. The $h_w$ values as read from these two figures at about 307 ± 1K are listed in Table 2 and are shown plotted in Figure 9. For zero water flow velocity the earlier measured $h_w$ values are also shown. The influence of water flow velocity on $h_w$ in the range of present measurements seem to be negligibly small as the scatter is always within the range of experimental uncertainty in $h_w$. The corresponding values of total gas holdup, $\bar{\epsilon}_g$, are also shown in Figure 9 and are reported in Table 2.

The data acquisition system (HP 3497A) used in the present measurements is a 5 1/2 digit digital voltmeter and 20 channel relay multiplexer assembly so that the thermocouples output can be measured in a chosen sequence. The system is remotely controlled by a HP 310 computer which is interfaced with a dual flexible disc drive, HP Thinkjet printer and HP Color Pro plotter. The thermocouple emf's are converted into temperature using adequate software and thence into heat transfer coefficient which are graphically displayed by the plotter. We have taken such data at the sampling rate of ten data points per minute and the same are shown in Figure 10, at various air velocities and for an aerated water column height of 170.2 cm. The column temperature exhibits a steady slow temperature rise over the period of 50 minutes. The rise depends on the gas velocity and the actual temperatures are shown in each case. It is important to note that the steady-state is reached in about four minutes and thereafter any variation in $h_w$ is attributed to the change in column temperature. It is also interesting to note that $h_w$ fluctuates continuously with time in a random fashion and the magnitude of maximum fluctuation increases with increase in air velocity. The magnitudes of these fluctuations are 6.6%, 5.3%. 7.2%, 9.0% and 9.4% at 6.86, 13.8, 20.9, 28.1 and 35.3 cm/s respectively. These data records revealed that the heat removal from the heater surface is most probably by the air-liquid dispersion elements which continuously visit the heater surface. This bathing of the surface is brought about by the turbulent nature of the air-water dispersion. To confirm whether the surface is covered by the discontinuous phase (air bubble) on a regular basis with a finite frequency or not, an experiment has been performed. It involved the measurement of the local temperature of the heater surface as a function of time over a period of 10 s at the rate of twenty readings per second. A pronounced variation of the local temperature with time and its periodicity will suggest the nature of phases in contact with the heater surface and their duration of stay and rate of replenishment i.e., their residence time and frequency.

Figure 11 shows our experimental findings at different air velocities when a constant power is fed to the heater. Also shown in this figure (curve a) is the variation of local temperature when the heater surface is at the column temperature but the air is being bubbled through the water column. The temperature variations of the curves (b, c and d) are to be evaluated in the background of variations implicit in curve a. It is clear that the local surface temperature does not exhibit wide fluctuations suggesting thereby that the nature of the phase in contact with it does not significantly change. In particular, the surface never sees the pure discontinuous phase, and the small fluctuations may be due to the different mix of pure phases (water and air) in the dispersion element visiting the heater surface. A partial confirmation to this proposed mechanism of heat transfer also comes from the results displayed in Figure 9. The air holdup increases monotonically with increasing air velocity, while the $h_W$ values tend to become constant at higher air velocities. This suggests that the role played by air velocity is primarily in churning and agitating the liquid. At low gas velocities, the liquid agitation increases with increase in gas velocity and hence $h_W$ increases with increase in gas velocity in the low gas velocity range. As the gas velocity is further increased the heat transfer rate becomes constant because any increase in the frequency of gas-liquid dispersion visit at the heat transfer surface does not significantly influence the heat removal rate in this gas velocity range. Any minor change in the heat transfer rate in this gas velocity range can also be balanced by the change in thermal properties of the dispersion due to changes in its composition as the gas velocity is increased. This conjectured mechanism of heat transfer from an immersed surface to the gas-liquid suspension in a bubble column will be further developed in our continuing work.

It is also considered desirable to investigate the dependence of heat transfer coefficient, $h_W$, on the value of thermal flux, $Q/A$, when all the other variables are held constant. We, therefore, measured the $h_W$ values for the air velocity of 34.4 cm/s, column temperature of about 312K when the heater is located 87.5 cm above the distributor. The electrical power supplied to the heater is varied between 0.456 to 0.943 kW. The measured $h_W$ values are listed in Table 3 and it is noticed that these do not vary in any systematic manner with the increase in thermal flux. The maximum variation in the $h_W$ values is also within the maximum uncertainty assigned to the measured $h_W$ values.

The measured uncertainty of our data is estimated to be about 4.5% on the basis of the following equations.

$$\frac{\delta h_w}{h_w} = \sqrt{\left(\frac{\delta Q}{Q}\right)^2 + \left(\frac{\delta(\Delta T)}{\Delta T}\right)^2 + \left(\frac{\delta A}{A}\right)^2}$$

where

$$\left(\frac{\delta Q}{Q}\right)^2 = \left(\frac{\delta Vo}{Vo}\right)^2 + \left(\frac{\delta I}{I}\right)^2,$$

$$\left(\frac{\delta \Delta T}{\Delta T}\right)^2 = \left(\frac{\delta T_s}{\Delta T}\right)^2 + \left(\frac{\delta T_c}{\Delta T}\right)^2,$$

and

$$\left(\frac{\delta A}{A}\right)^2 = \left(\frac{\delta L}{L}\right)^2 + \left(\frac{\delta D}{D}\right)^2,$$

Here $\delta h_W$, $\delta Q$, $\delta(\Delta T)$ and $\delta(A)$ represent the error in $h_W$, Q, $\Delta T$ and A respectively. $\Delta T = T_S - T_C$ is the temperature difference between the temperatures of the heater surface ($T_S$) and the air-water dispersion ($T_C$). The electrical power (Q) supplied to the heater is the product of the current (I) through it and voltage (Vo) applied across it. The heater area (A) is $\pi$DL where D is the diameter and L is the length of the heater section of the heat transfer probe.

A seven-probe bundle is designed, fabricated and is ready for use.

TASK 3

The design, fabrication and installation work on the larger 0.305 m diameter column has progressed and it is expected that the various flow loops and measuring circuits will be completed shortly. In particular, the air supply line is completed as also the circuit for measuring pressure profile along the column. The latter consists of four air purge meters, twelve on-off valve, four trap bottles, and four mercury manometers. This arrangement enables to establish the pressure drop across three sections of the column as well as across the whole column. A pressure transducer with a digital monitor is also installed as an alternative arrangement to manometers to measure the pressure distribution.

A heat transfer probe of 19 mm diameter and of the same general design as used in conjunction with the small 10.8 cm diameter column is designed for use with the larger (0.305 m) column. It is in the advanced stage of fabrication. Three three-arm clamps, each having two telescopic arms, have been constructed with great care and precision to ensure stable and accurate axial positioning of the probe in the column. A diverger section for the top end of the column with special provision to mount the upper end of the probe is designed and its fabrication will start soon as the materials required in its construction have been procured.

To energize the electrical heater in the probe a special electrical circuit is assembled on an aluminum panel box comprising of a selector switch, digital multimeter, and connectors. To measure the column and probe surface temperatures by the copper constantan thermocouples, a twenty jack panel board is prepared and installed. The remaining measurement system remains the same as used in conjunction with the smaller bubble column.

TASK 4

We now present an interpretation of our experimental air holdup data for different operating conditions in terms of available correlations. In the progress report for the month of November 1987, we reported the gas holdup data for the air-water system as a function of air velocity at a temperature of 297 K. The liquid velocity was zero so that the operation may be referred as semi-batch. These data were taken for increasing air flow velocity and then for decreasing air flow velocity. In all cases a constant expanded height of the water column as 170.18 cm is maintained and the corresponding water column height upon cessation of air flow is measured. From these measurements the average air holdup, $\bar{\epsilon}_g$, is computed. The data are shown in Figure 12. A pronounced maximum and minimum are observed for increasing air velocity while a monotonic variation of increasing $\bar{\epsilon}_g$ with increasing U is found for decreasing air velocity. This hysterisis effect has been observed by other workers also[1-4] and is primarily due to the formation and accumulation of foam at the top of air-water dispersion and secondarily due to foam accumulation in the column. Maruyama et al.[2] based on their work in a twodimensional column with a rectangular cross section of 30 cm x 1 cm and a height of 130 cm have attributed such a dependence of $\bar{\epsilon}_g$ on U to different liquid flow patterns. Three regimes of operation viz., uniform bubbling, transition and liquid circulation have been proposed and these are encountered as the air velocity is increased. In the transition regime local liquid circulation near the side walls and gross liquid circulation may occur depending upon the gas velocity. At the maximum holdup, a symmetrical two-loop circulation pattern, upward near the middle and downward near the side wall, is observed. A monotonic decrease in $\bar{\epsilon}_g$ values is observed when the air velocity is decreased.

Hughmark[5,6,11] proposed the following correlation for air-water system

$$\bar{\epsilon}_g = \frac{1}{2 + (0.35/U)} \tag{1}$$

Modifications of this correlation have been proposed for other liquids[5] and for three-phase systems[7].

Akita and Yoshida[8] recommended a general correlation for gas-liquid systems including air-water as

$$\bar{\epsilon}_g / \left(1 - \bar{\epsilon}_g\right)^4 = 0.20\, Bo^{1/8} Ga^{1/12} Fr \tag{2}$$

where

$$\text{Biot number (Bo)} = \left(g D_c^2 \rho_L / \sigma\right) \tag{3}$$

$$\text{Galileo number (Ga)} = \left(g D_c^3 / \nu_L^2\right) \tag{4}$$

and $$\text{Froude number (Fr)} = U / \sqrt{g D_c} \tag{5}$$

Here $D_c$ is the column diameter, $\rho_L$ is the liquid density, $\sigma$ is the surface tension of the liquid, $\nu_L$ is the kinematic viscosity of the liquid, and g is the acceleration due to gravity. All quantities are in SI unit system. Recently Sada et al.[9] has proposed the following modification to the above correlation of Equation (2) by including a density ratio term:

$$\bar{\epsilon}_g / \left(1 - \bar{\epsilon}_g\right)^4 = 0.32\, Bo^{0.121} Ga^{0.086} \left(\rho_g / \rho_L\right)^{0.068} Fr \tag{6}$$

Here $\rho_g$ is the gas density in SI units. The predictions based on equations (2) and (6) for air-water system differ from each other by less than 0.05 percent.

Kumar et al.[10] proposed

$$\epsilon_g = 0.728\,U' - 0.485\,U'^2 + 0.0975\,U'^3 \tag{7}$$

where

$$U' = U\left[\rho_L^2 / \left\{\sigma\left(\rho_L - \rho_g\right)g\right\}\right]^{1/4} \tag{8}$$

Here all the quantities are in SI units.

According to Hikita et al.[11]

$$\epsilon_g = 0.672\left(U\mu_L/\sigma\right)^{0.578}\left(\mu_L^4 g/\rho_L\sigma^3\right)^{-0.131}\left(\rho_g/\rho_L\right)^{0.062}\left(\mu_g/\mu_L\right)^{0.107} \tag{9}$$

Here all quantities are in S.I. units, $\mu_L$ and $\mu_g$ are the viscosities of liquid and gas respectively.

Reilly et al.[12] have proposed

$$\epsilon_g = 0.009 + 296U^{0.44}\rho_L^{-0.98}\sigma^{-0.16}\rho_g^{0.19} \tag{10}$$

Hills[13] has proposed that for air-water system, the gas holdup is given by

$$\epsilon_g = U\left[0.24 + 4.0\,\epsilon_g^{1.72}\right]^{-1} \tag{11}$$

Computed values of gas holdup as obtained on the basis of the relations of equations (1) through (11) are shown in Figure 12 along with our experimental data. The data corresponding to increasing air velocity is qualitatively reproduced by the correlation of Kumar et al.[10] only. The correlations of Hughmark[5], and Reilly et al.[12] are considered adequate in predicting the present gas holdup data as a function of decreasing air velocity. It is also to be noted that the nonmonotonic behavior of air holdup for increasing air velocity is only qualitatively reproduced by the correlation of Kumar et al.[10]

The above discussion is for an upward flow of gas through a liquid column with zero flow velocity. In Figure 13 are also shown the gas holdup data for three water flow velocities, V, cocurrent with air velocities. In this range of water velocities (0.373 to 0.892 cm/s), $\bar{\epsilon}_g$ is not dependent on V. For such a cocurrent two-phase flow, the gas holdup, $\bar{\epsilon}'_g$, is correlated by Hughmark[5] on the basis of the following relation:

$$U = \bar{\epsilon}_g \left[ \frac{U}{\bar{\epsilon}'_g} - \frac{V}{1 - \bar{\epsilon}'_g} \right] \qquad (12)$$

Here $\bar{\epsilon}_g$ is to be computed from equation (1). Hills[13] on the other hand proposed that as long as $V \leq 0.3$ m/s, $\bar{\epsilon}_g$ may be computed from the following relation:

$$\left( U/\bar{\epsilon}'_g \right) - \left[ V/\left( 1 - \bar{\epsilon}'_g \right) \right] = 0.24 + 4.0\, \bar{\epsilon}'^{\,1.72}_g \qquad (13)$$

Comparison of $\bar{\epsilon}'_g$ data for the three liquid velocities with the predictions based on equations (12) and (13) is shown in Figure 13 as a function of air velocity.

Additional data of gas holdup for the two-phase cocurrent flow are taken and the same are displayed in Figures 14 and 15. These also correspond to the case where in the column a 19.0 mm diameter cylindrical heat transfer probe is introduced along its axis. To avoid overcrowding of the data, $\bar{\epsilon}'_g$ values are displaced upward by a constant amount. These two sets of data are not in complete qualitative agreement with each other and it is attributed to the presence of varying amounts of trace surfactants in the system. Nevertheless the qualitative dependence of $\bar{\epsilon}'_g$ on U and V mentioned above is displayed by these sets of data also. Shown in Figures 14 and 15 are also the predictions of $\bar{\epsilon}'_g$ based on the correlations of equations (11) and (12).

On the whole we find that the observed dependence of air holdup on air velocity is not even qualitatively reproduced by the two correlations. The correlation of equation (12) due to Hughmark[5,6,11] underpredicts the experimental data of Figure 14 while overpredicts that of Figure 15. The reproduction of experimental data of Figure 14 is relatively better by the correlation of Hills[13], equation (13). On the other hand it reproduces rather poorly the experimental data of Figure 15. We infer that these correlations are reasonable in estimating the gas holdup within an uncertainty of about twenty percent and for precise knowledge direct measurements should be preferred. The differences in the values are primarily due to the changing physical properties of the system brought about by the changes in the chemical composition of the phases involved.

NOMENCLATURE

| | | |
|---|---|---|
| $A$ | = | Area of heat transfer, $m^2$ |
| Bo | = | Biot number, defined by equation (3) |
| $D$ | = | Diameter of the heat-transfer probe, m |
| $D_c$ | = | Column diameter, m |
| Fr | = | Froude number, defined by equation (5) |
| Ga | = | Galileo number, defined by equation (4) |
| $g$ | = | Acceleration due to gravity, $m/s^2$ |
| $h_w$ | = | Heat-transfer coefficient, $kW/m^2K$ |
| $I$ | = | Current through the heater, A |
| $L$ | = | Length of the heat-transfer probe, m |
| $Q$ | = | Electrical power supplied to the heater, kW |
| $T_c$ | = | Temperature of the air-water dispersion, K |
| $T_s$ | = | Temperature of the heater surface, K |
| $U$ | = | Superficial gas flow velocity, m/s |
| $U'$ | = | Defined by equation (8) |
| $V$ | = | Superficial water flow velocity, m/s |
| $V_o$ | = | Voltage applied across the heater, V |
| $\delta A$ | = | Error in area of heat transfer, $m^2$ |
| $\delta D$ | = | Error in diameter of heat-transfer probe, m |
| $\delta h_w$ | = | Error in heat transfer coefficient, $kW/m^2K$ |
| $\delta I$ | = | Error in current through the heater, A |
| $\delta L$ | = | Error in length of the heat-transfer probe, m |
| $\delta Q$ | = | Error in electrical power supplied to the heater, kW |
| $\Delta T$ | = | Temperature difference between the temperatures of the heater-surface and the air-water dispersion, K |
| $\delta \Delta T$ | = | Error in the temperature difference between the temperatures of the heater surface and the air-water dispersion, K |
| $\delta T_c$ | = | Error in the temperature of air-water dispersion, K |
| $\delta T_s$ | = | Error in the temperature of the heater surface, K |
| $\bar{\varepsilon}_g$ | = | Average holdup with $V = 0$, - |
| $\bar{\varepsilon}'_g$ | = | Average air holdup with $V > 0$, - |

| | | |
|---|---|---|
| $\mu_g$ | = | Viscosity of the air, kg/ms |
| $\mu_L$ | = | Viscosity of the water, kg/ms |
| $v_L$ | = | Kinematic viscosity of the water, $m^2/s$ |
| $\rho_g$ | = | Density of the air, $kg/m^3$ |
| $\rho_L$ | = | Density of the water, $kg/m^3$ |
| $\sigma$ | = | surface tension of water, N/m |

## References


1. J. Zahradnik and F. Kastanek, Gas Holdup in Uniformly Aerated Bubble Column Reactors, Chem. Eng. Commun. 3, 413-429, 1979.

2. T. Maruyama, S. Yoshida and T. Mizushina, The Flow Transition in a Bubble Column, J. Chem. Eng. Japan, 14, 352-357, 1981.

3. D.B. Bukur and J.G. Daly, Gas Holdup in Bubble Columns for Fischer-Tropsch Synthesis, Chem. Eng. Sci. 42, 2967-2969, 1987.

4. D.B. Bukur, D. Petrovic and J.G. Daly, Flow Regime Transitions in a Bubble Column with a Paraffin Wax as the Liquid Medium, Ind. Eng. Chem. Res. 26, 1087-1092, 1987.

5. G.A. Hughmark, Holdup and Mass Transfer in Bubble Columns, Ind. Eng. Chem. Process Des. Dev. 6, 218-220, 1967.

6. Y.T. Shah, B.G. Kelkar, S.P. Godbole and W.D. Deckwer, Design Parameters Estimations for bubble Column Reactors, AIChE J 28, 353-379, 1982.

7. D.N. Smith, W. Fuchs, R.J. Lynn and D.H. Smith, Bubble Behavior in a Slurry Bubble Column Reactor Model, Chemical and Catalytic Reactor Modeling, ACS Symp. Series No. 237, M.P. Dudokovic and P.L. Mills (Eds.), 125-147, 1984.

8. K. Akita and F. Yoshida, Gas Holdup and Volumetric Mass Transfer Coefficient in Bubble Columns, Ind. Eng. Chem. Process Des. Dev. 12, 76-80, 1973.

9. E. Sada, S. Katoh, H. Yoshii, T. Yamanishi and A. Nakanishi, Performance of the Gas Bubble Column in Molten Salt Systems, Ind. Eng. Chem. Process Des. Dev. 23, 151-154, 1984.

10. A. Kumar, T.T. Dagaleesan, G.S. Laddha and H.E. Hoelscher, Bubble Swarm Characteristics in Bubble Columns, Canadian J. Chem. Eng. 54, 503-508, 1976.

11. H. Hikita, S. Asai, K. Tanigawa, K. Segawa and M. Kitao, Gas Holdup in Bubble Columns, Chem. Eng. J. 20, 59-67, 1980.

12. I.G. Reilly, D.S. Scott, T. De Bruijn, A. Jain and J. Piskorz, A Correlation for Gas Holdup in Turbulent Coalescing Bubble Columns, Canadian J. Chem. Eng. 64, 705-717, 1986.

13. J.H. Hills, The Operation of a Bubble Column at High Throughputs I. Gas Holdup Measurements, Chem. Eng. J. 12, 89-99, 1976.

Table 1. Values of $h_w$ and $\bar{\epsilon}_g$ at 315 ± 1K as a function of air velocity for different heater locations in the column.

| Air Velocity, V | Lower (H = 57.2 cm) | | Middle (H = 87.5 cm) | | Middle (H = 87.5cm) | | Upper (H = 118.1 cm) | |
|---|---|---|---|---|---|---|---|---|
| cm/s | $h_w$, kw/m$^2$K | $\bar{\epsilon}_g$ | $h_w$, kw/m$^2$K | $\bar{\epsilon}_g$ | $h_w$, kw/m$^2$K | $\bar{\epsilon}_g$ | $h_w$, kw/m$^2$K | $\bar{\epsilon}_g$ |
| 3.39 | 4.62 | 0.074 | 4.36 | 0.071 | 4.45 | 0.071 | 4.48 | 0.088 |
| 6.86 | 5.08 | 0.190 | 5.08 | 0.148 | 5.20 | 0.138 | 5.38 | 0.131 |
| 10.3 | 5.56 | 0.181 | 5.52 | 0.173 | 5.51 | 0.184 | 5.56 | 0.193 |
| 13.8 | 5.82 | 0.212 | 5.80 | 0.202 | 5.66 | 0.231 | 5.70 | 0.180 |
| 17.3 | 6.02 | 0.241 | 5.77 | 0.224 | 5.78 | 0.237 | 5.86 | 0.229 |
| 20.9 | 6.08 | 0.224 | 6.01 | 0.240 | 6.01 | 0.261 | 6.00 | 0.274 |
| 24.5 | 6.20 | 0.294 | 6.18 | 0.262 | 6.18 | 0.276 | 6.08 | 0.320 |
| 28.1 | 6.12 | 0.306 | 6.04 | 0.301 | 6.05 | 0.307 | 6.05 | 0.346 |
| 31.7 | 6.20 | 0.340 | 6.12 | 0.336 | 6.12 | 0.331 | 6.04 | 0.337 |
| 35.3 | 6.18 | 0.397 | 6.20 | 0.339 | 6.19 | 0.394 | 6.10 | 0.372 |

Table 2: Values of $h_w$ (kW/m$^2$K) and $\bar{\epsilon}'_g$ (-) at the column temperature of 307 ± 1K as a function of U(m/s) at different V(mm/s)

| U | V = 0.0 | | V = 6.8 | | V = 11.9 | |
|---|---|---|---|---|---|---|
| | $h_w$ | $\bar{\epsilon}_g$ | $h_w$ | $\bar{\epsilon}'_g$ | $h_w$ | $\bar{\epsilon}'_g$ |
| 0.135 | 5.31 | 0.202 | - | - | 5.22 | 0.233 |
| 0.203 | 5.62 | 0.240 | 5.64 | 0.305 | 5.76 | 0.295 |
| 0.273 | 5.79 | 0.301 | 5.96 | 0.338 | 5.72 | 0.336 |
| 0.344 | 5.72 | 0.339 | 5.92 | 0.379 | 5.88 | 0.361 |

Table 3: Experimental values of $h_w$ (kW/m$^2$K) for different electrical power input to the heater, Q(kW), at a fixed column temperature $T_c$(K).

| $T_c$ | Q | $h_w$ |
|---|---|---|
| 312.7 ± 0.8 | 0.4560 | 5.915 ± 0.089 |
| 312.6 ± 0.6 | 0.6072 | 5.779 ± 0.216 |
| 313.8 ± 1.1 | 0.8113 | 5.937 ± 0.082 |
| 312.0 ± 1.4 | 0.9430 | 6.003 ± 0.340 |

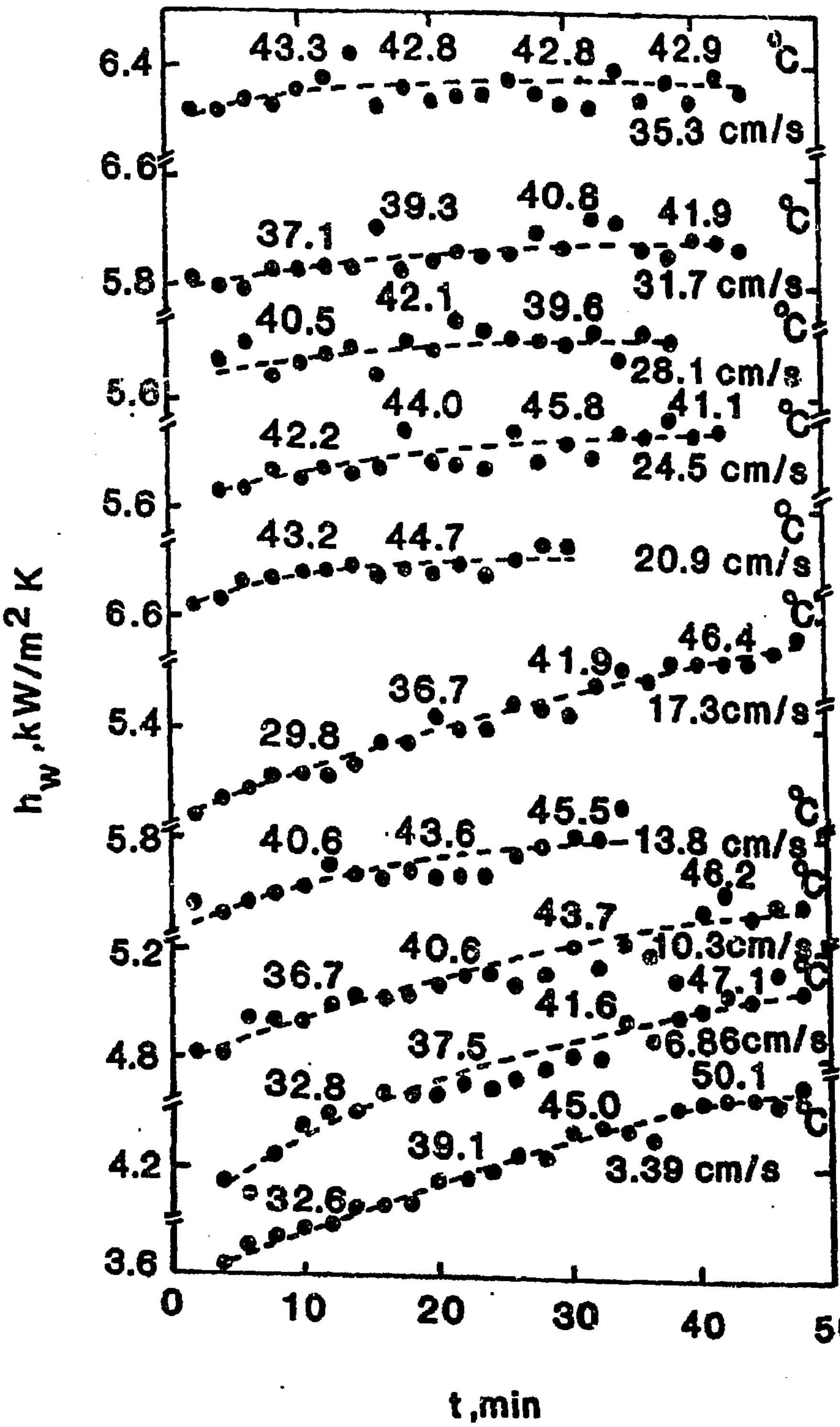


Figure 2. Variation of the heat transfer coefficient with time at different air velocities. Heater is located at 87.5 cm above the distributor plate (middle region).

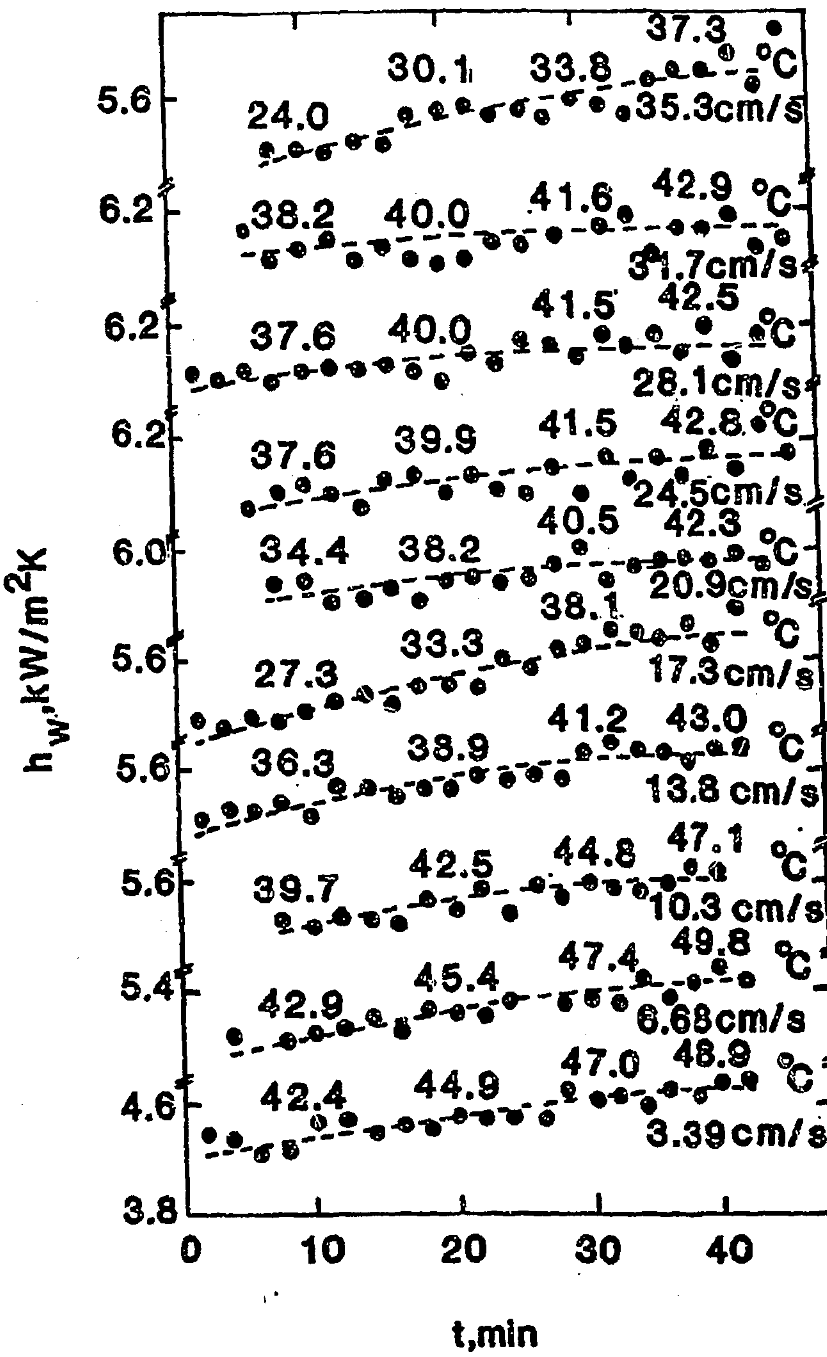


Figure 3. Variation of the heat transfer coefficient with time at different air velocities. Heater is located at 87.5 cm above the distributor plate (middle region).

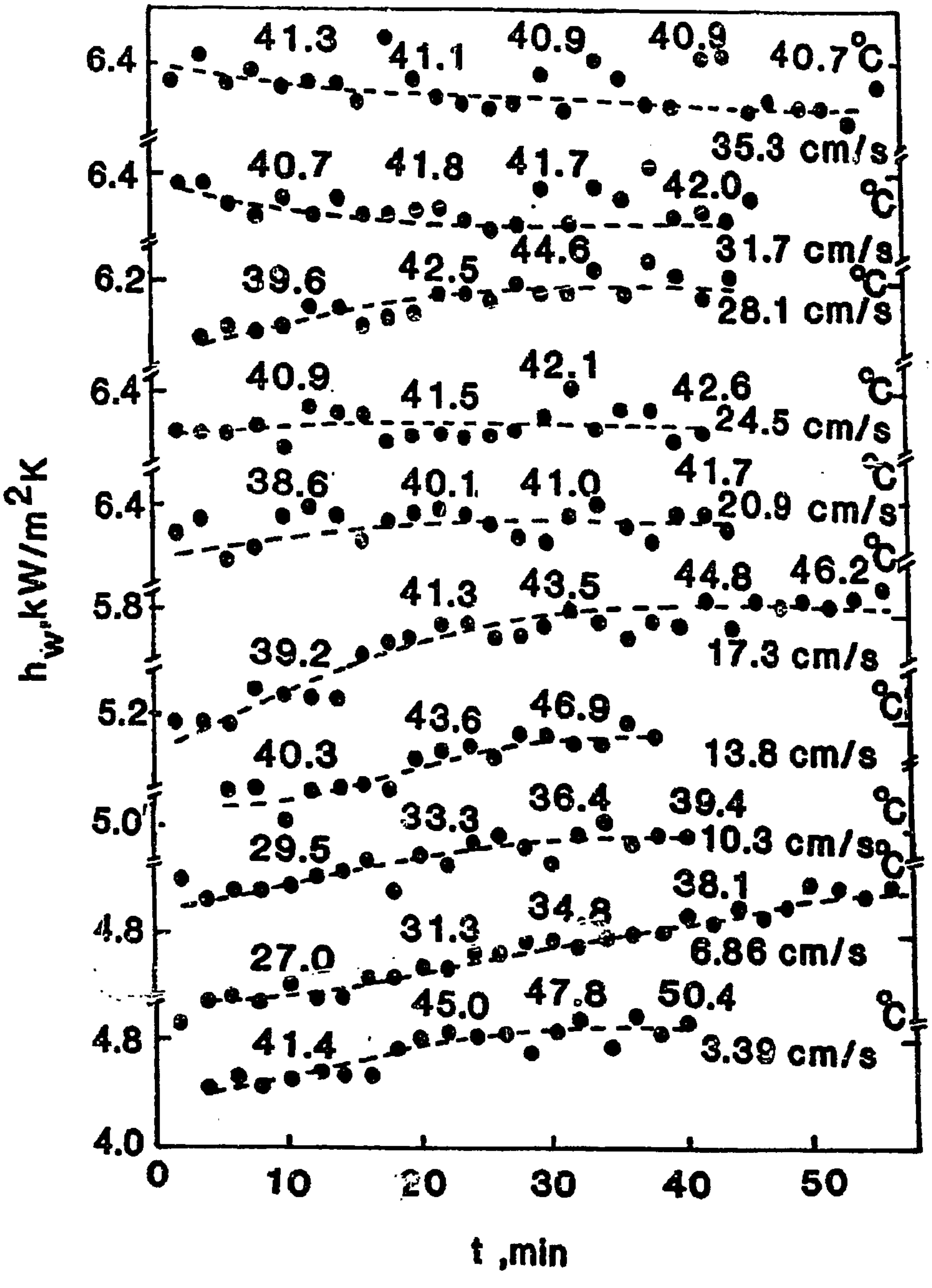


Figure 4. Variation of the heat transfer coefficient with time at different air velocities. Heater is located at 57.2 cm above the distributor plate (lower region).

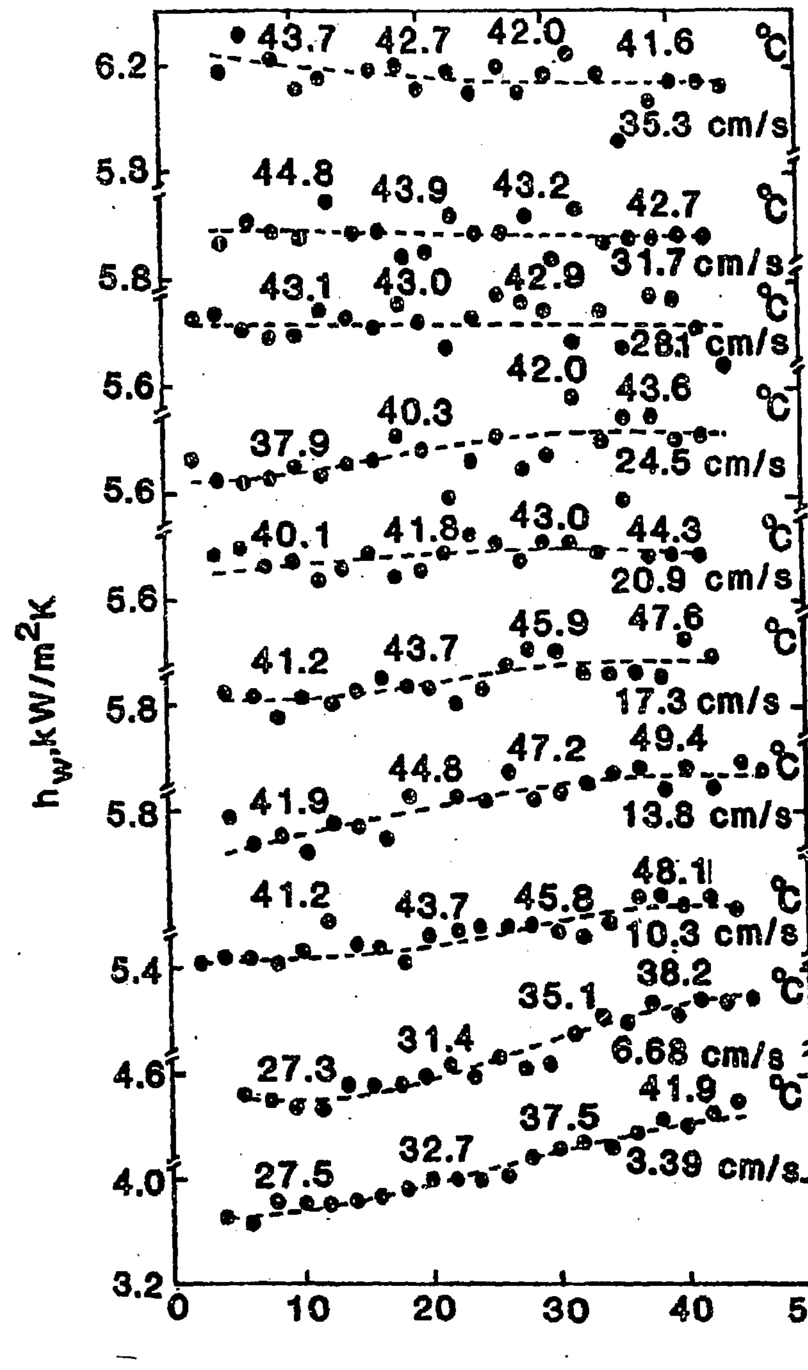


Figure 5. Variation of the heat transfer coefficient with time at different air velocities. Heater is located at 118.1 cm above the distributor plate (upper region).

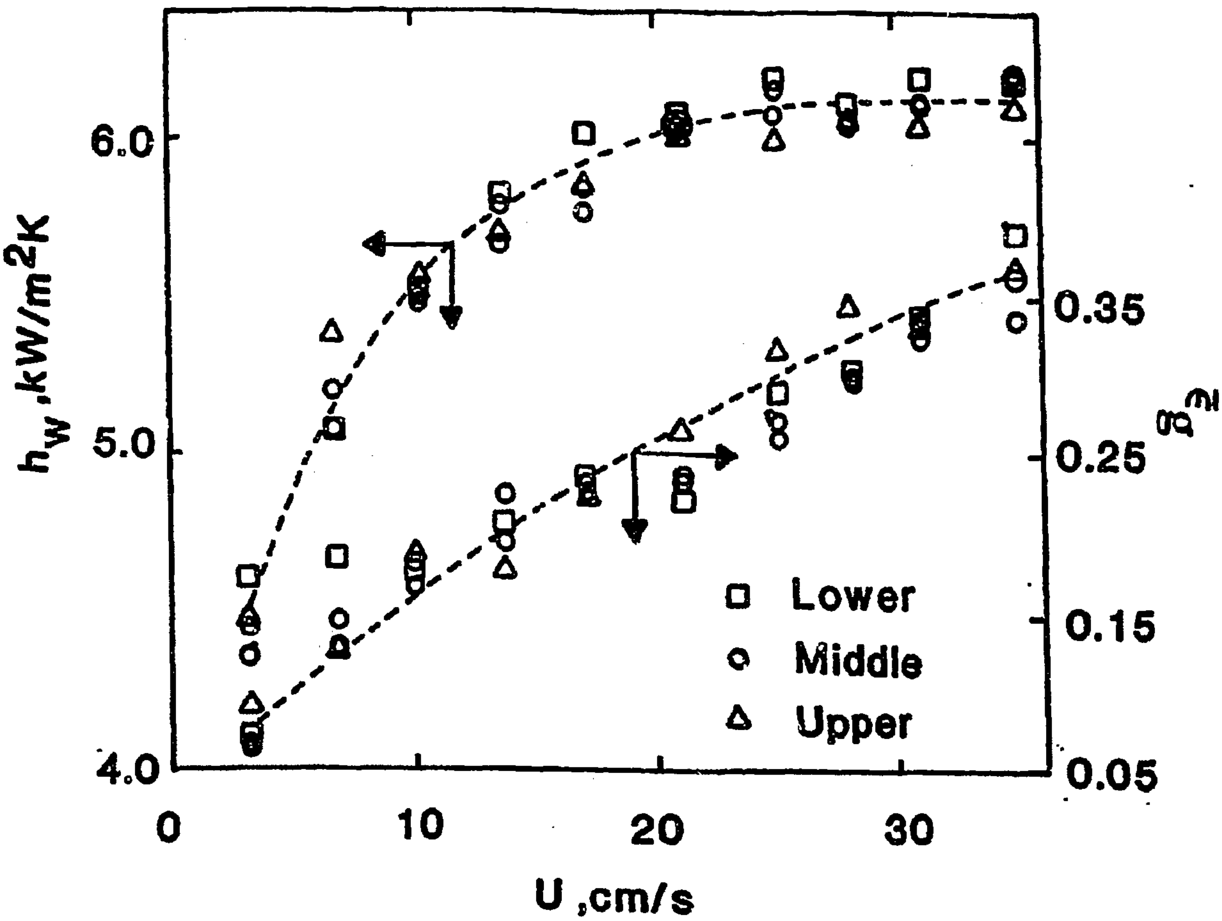


**Figure 6.** Variation of the heat transfer coefficient and average air holdup as a function of air velocity for three heater locations in the column.

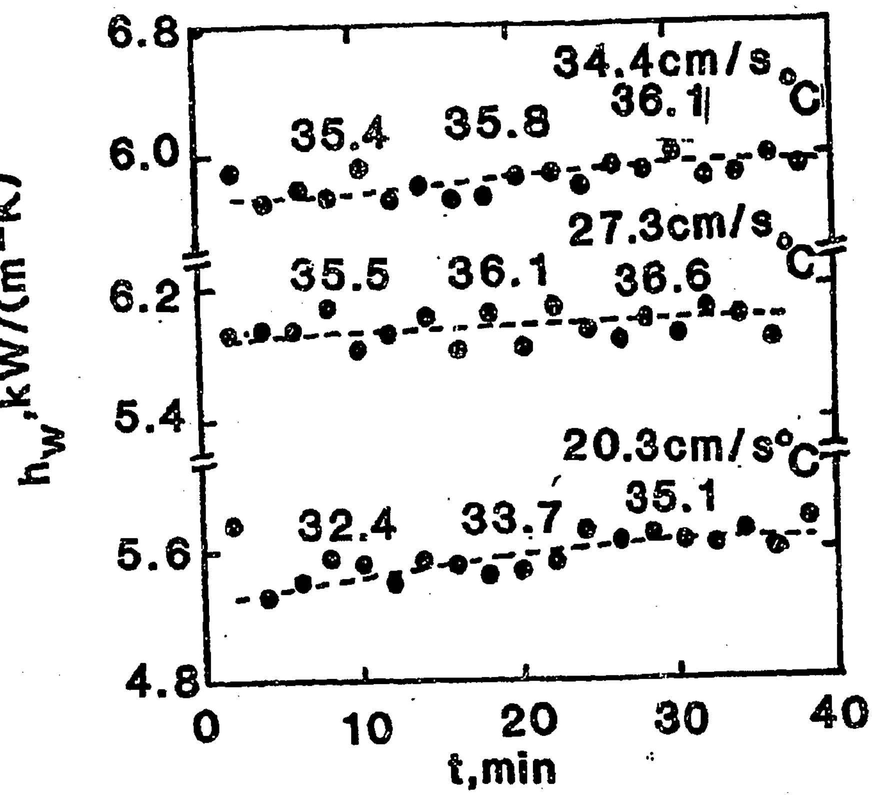


Figure 7. Variation of heat transfer coefficient ($h_w$) with time (t) at the water flow velocity (V) of 6.8 mm/s for different air velocities (U).

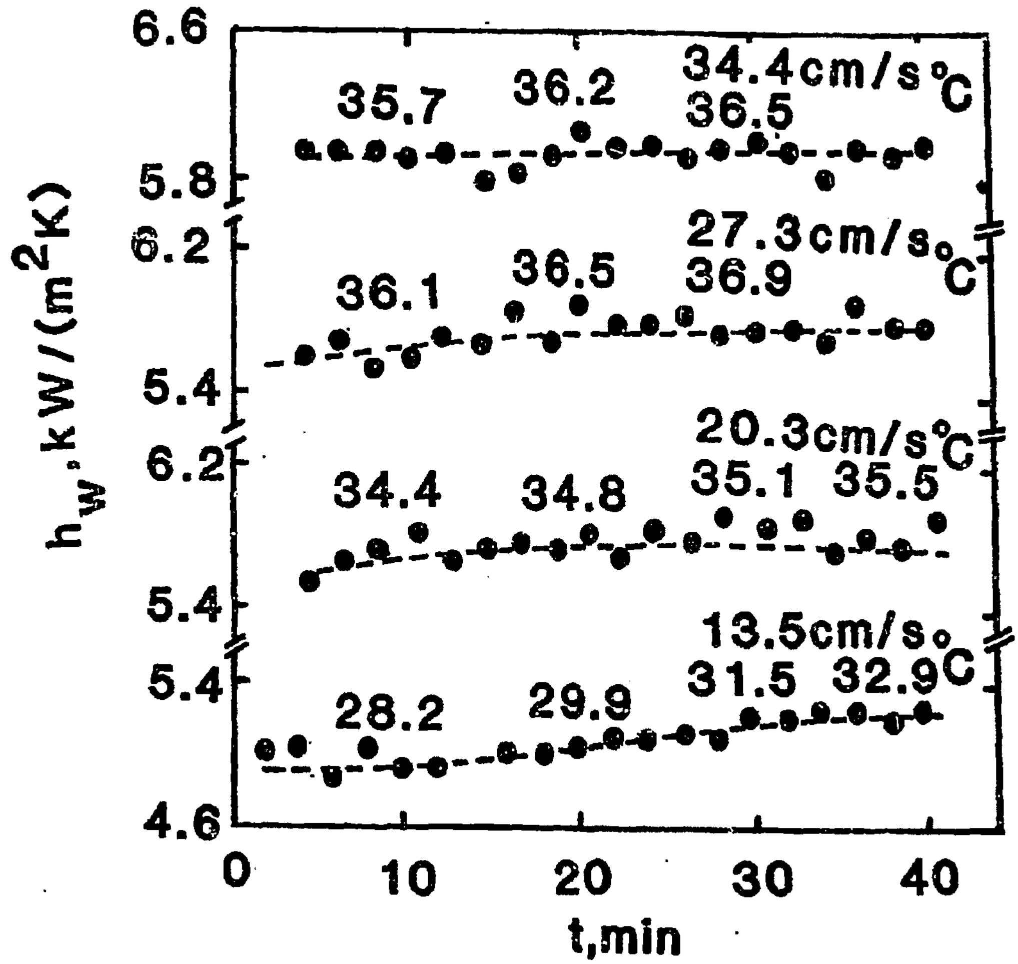


Figure 8. Variation of heat transfer coefficient ($h_w$) with time (t) at the water flow velocity (V) of 11.9 mm/s for different air velocities (U).

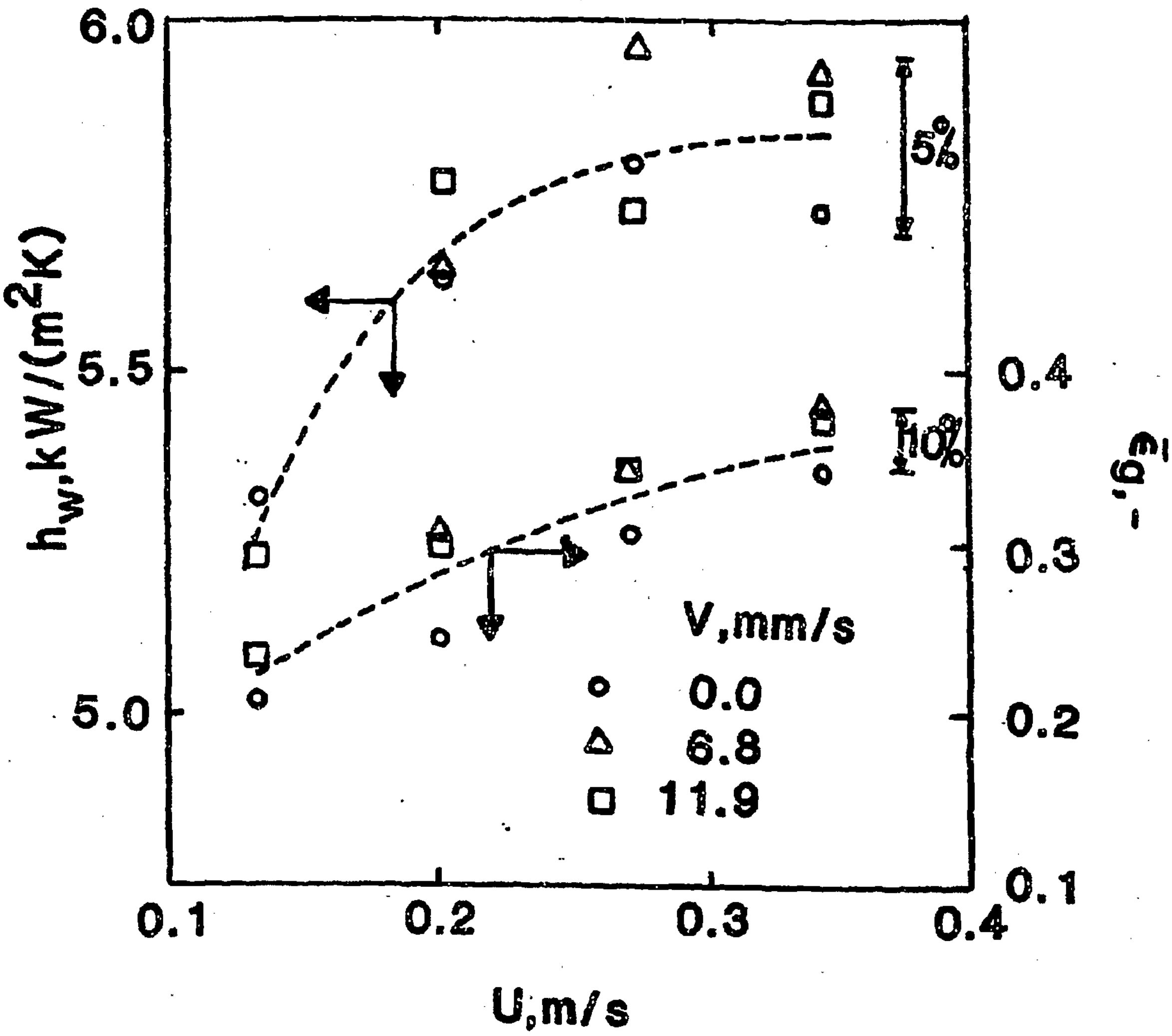


Figure 9. Variation of heat transfer coefficient ($h_W$) at 307 K with air velocity (U) at different water flow velocities (V).

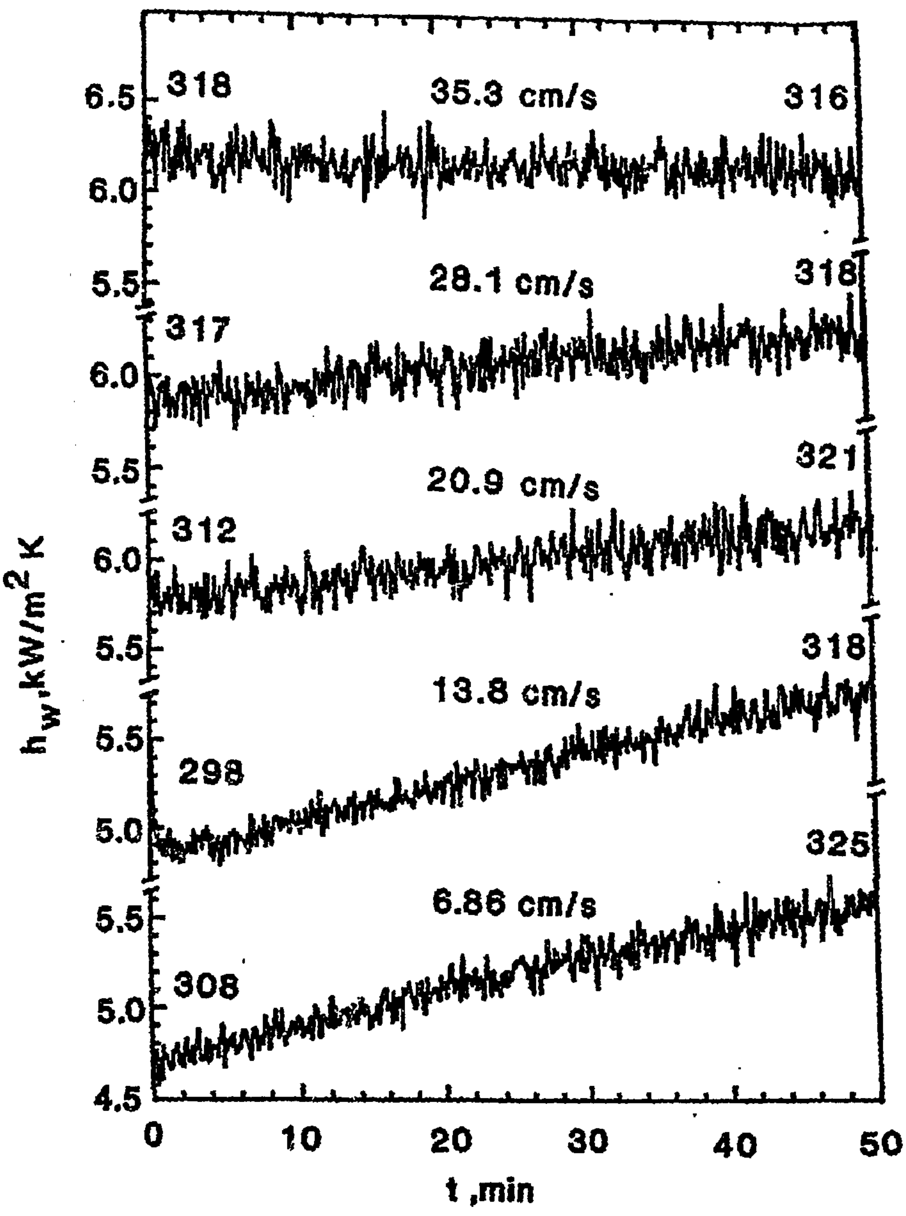


Figure 10. Variation of heat transfer coefficient ($h_w$) with time (t) at various air velocities.

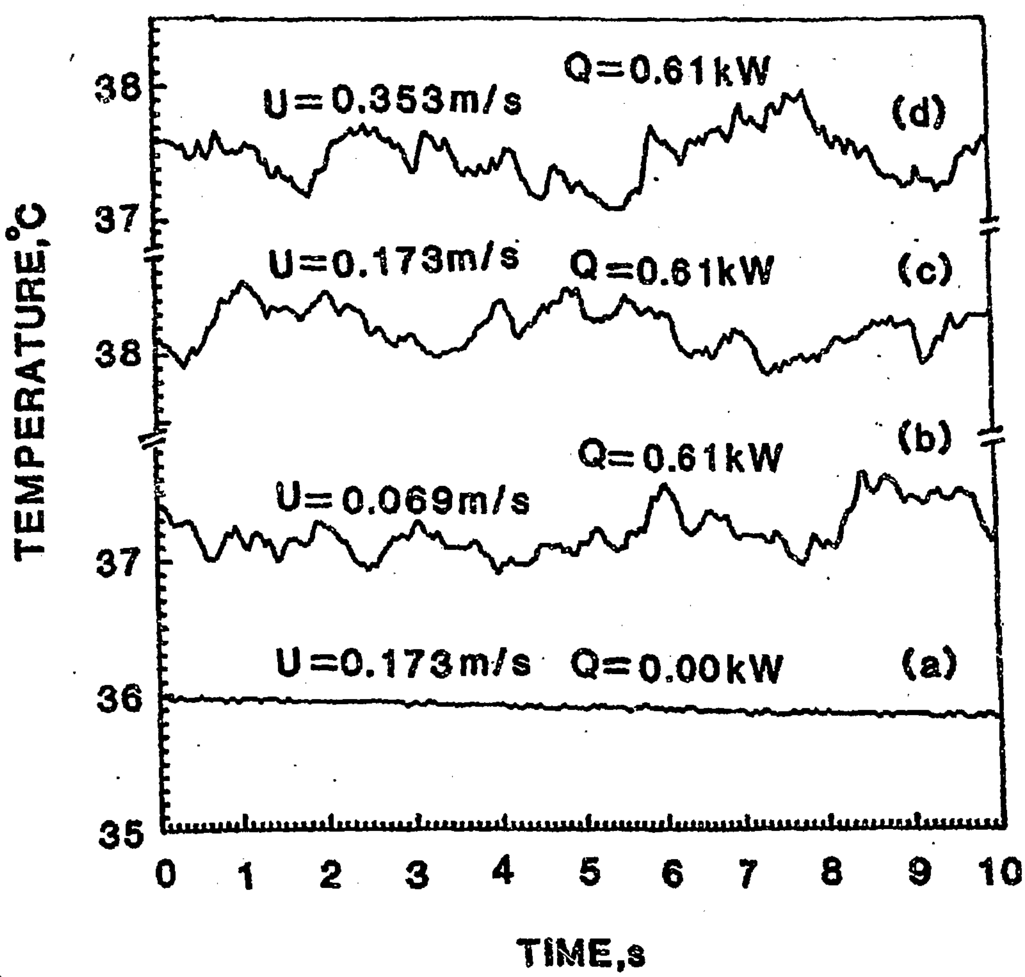


Figure 11. Variation of local temperature of heater surface with time at various air velocities.

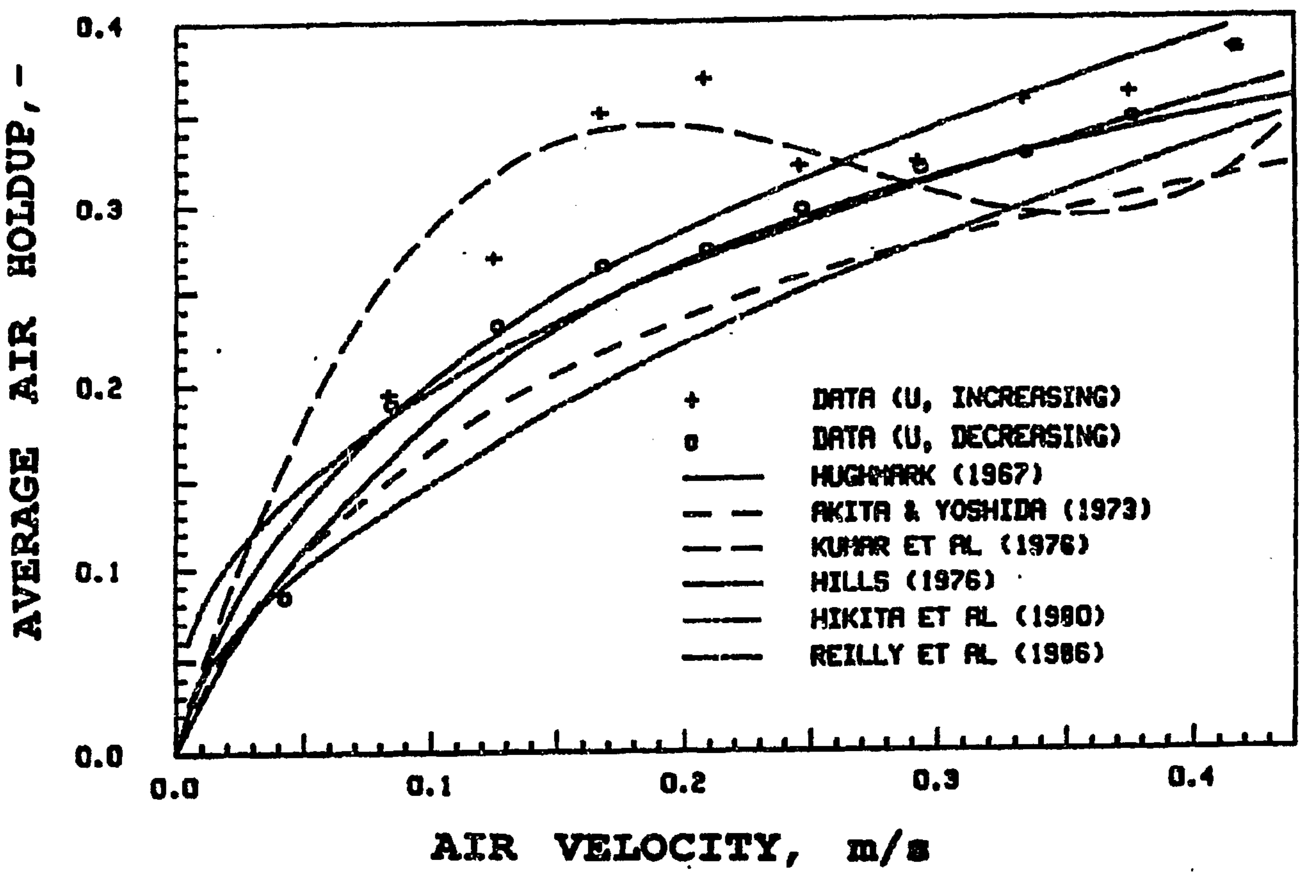


Figure 12. Comparison of experimental average air holdup as a function of air velocity for air-water system in the semi-batch mode with the predictions based on different correlations.

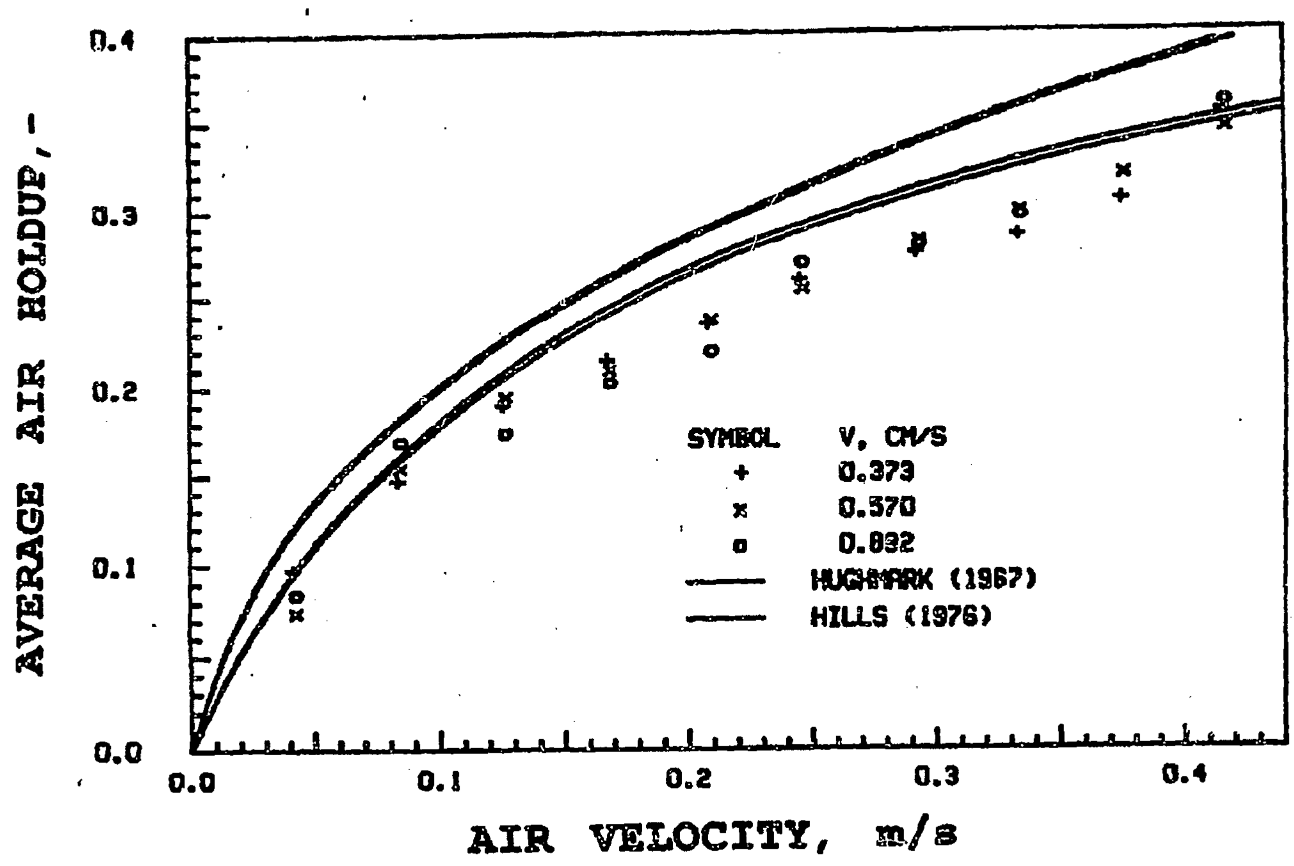


Figure 13. Comparison of experimental average air holdup as a function of air velocity for air-water system in the continuous mode with the predictions based on two correlations.

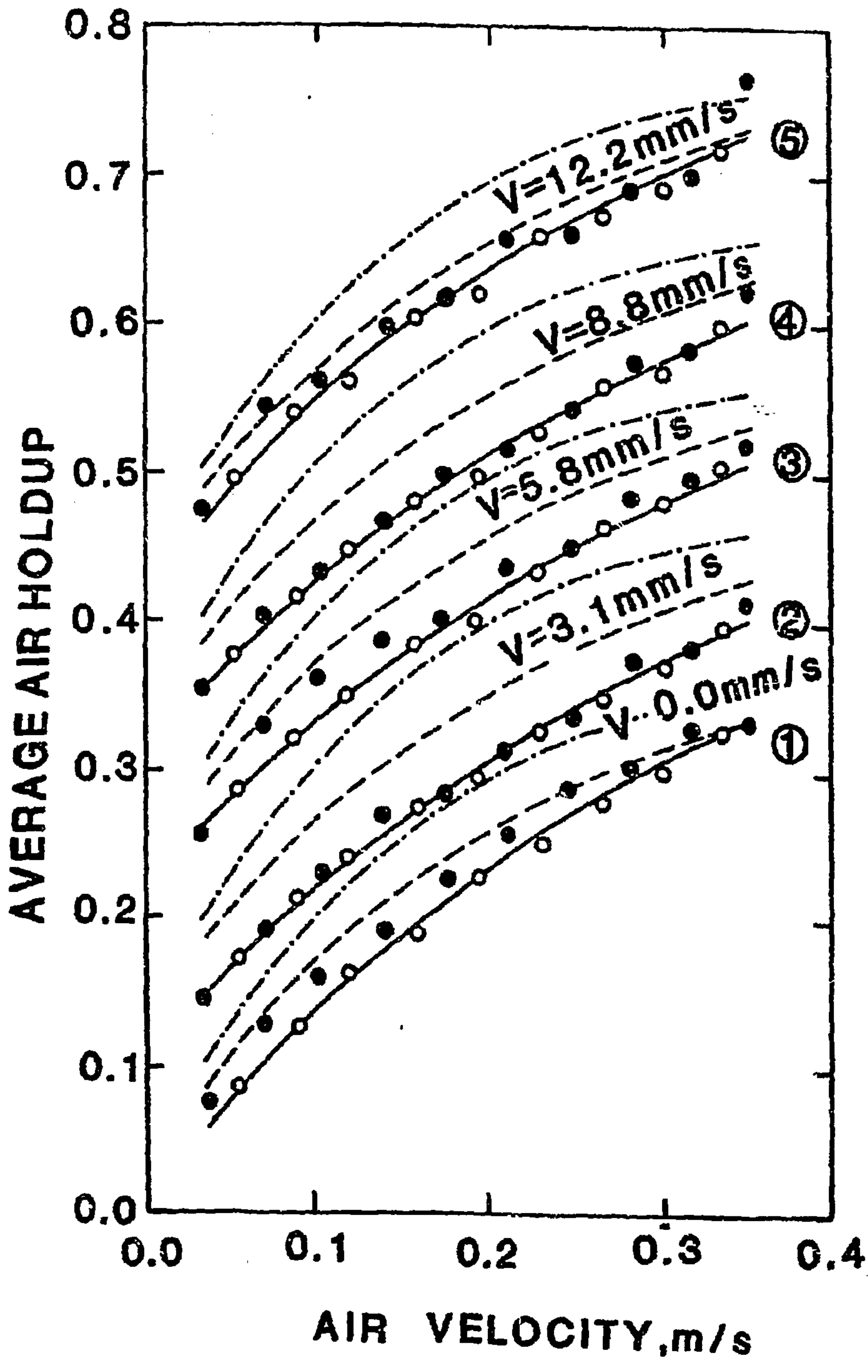


Figure 14. Variation of average air holdup as a function of increasing (●) and decreasing (O) air velocity for different liquid velocities (V) in the column with a coaxial heat transfer probe. Ordinates corresponding to 2, 3, 4 and 5 are shifted by 0.1, 0.2, 0.3 and 0.4 respectively. Continuous curves are smooth plots through the data points for decreasing gas velocity. Dashed and dot-dashed curves are based on equations (12) and (13) respectively.

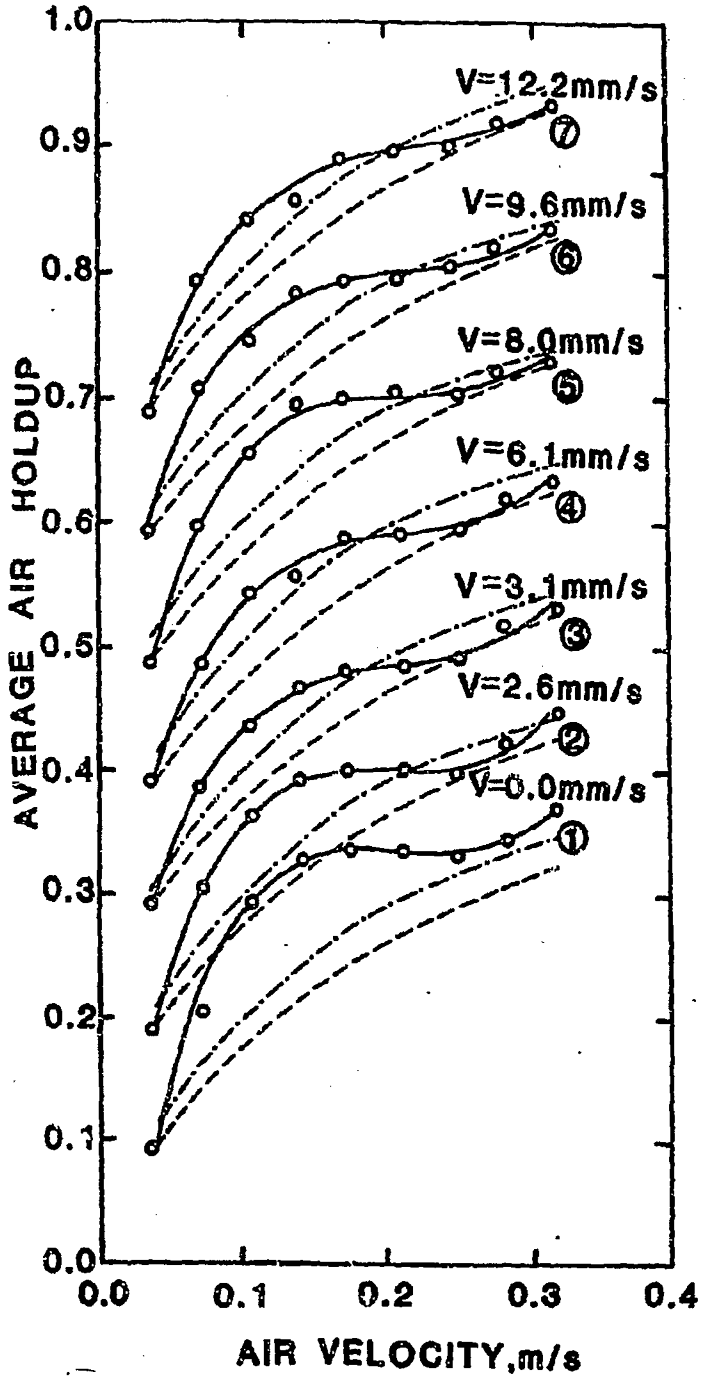


Figure 15. Variation of average air holdup as a function of decreasing air velocity for different liquid velocities (V) in the column with a coaxial heat transfer probe. Ordinates corresponding to 2, 3, 4, 5, 6 and 7 are shifted by 0.1, 0.2, 0.3, 0.4, 0.5 and 0.6 respectively. Continuous, dashed and dot-dashed curves are based on experimental data points, equations (12) and (13) respectively.

U.S. DEPARTMENT OF COMMERCE
Technology Administration
National Technical Information Service
Springfield, VA 22161 (703) 605-6000